

Transition metal impurities in Ge: Chemical trends and codoping studied by electronic structure calculations

A. Continenza, G. Profeta, and S. Picozzi

CASTI–Istituto Nazionale di Fisica della Materia (INFN/CNR) and Dipartimento di Fisica, Università degli Studi di L'Aquila, 67010 Coppito (L'Aquila), Italy

(Received 15 July 2005; revised manuscript received 28 November 2005; published 24 January 2006)

Ab initio electronic structure calculations within density functional theory have been performed to study the structural, electronic, and magnetic properties of transition metal impurities into a Ge matrix. We examine impurities of single isolated transition metal (TM) over the 3d series (TM=V, Cr, Mn, Fe, Co, Ni), occupying the substitutional and interstitial sites and interpret the electronic and magnetic properties in terms of a simple analysis based on atomic orbitals and electron filling. We show that Mn is indeed the most promising TM dopant to make Ge suitable for spintronic applications since it would grant ferromagnetic alignment, rather high local magnetic moment and hole doping. Then, we study the tendency of the most interesting TM impurities to cluster in the Ge matrix and investigate the case of (Mn,Co) and (Mn,Cr) codoping in Ge, both experimentally achieved. Analyzing the structural, electronic, and magnetic properties and giving insights regarding the expected solubility and the properties of the alloys, we find that while Mn impurities show a tendency to cluster, the presence of Co and overall Cr could favor a more uniform TM impurity distribution. However, both Co and Cr result to be far less efficient than Mn in promoting ferromagnetic alignment and high magnetic moment.

DOI: [10.1103/PhysRevB.73.035212](https://doi.org/10.1103/PhysRevB.73.035212)

PACS number(s): 75.50.Pp, 71.55.Cn, 71.55.-i, 71.15.Mb

I. INTRODUCTION

Great interest has been recently devoted to magnetic semiconductors based on III-V compounds where ferromagnetic coupling arises thanks to incorporation of magnetic impurities, mainly Mn, into the semiconductor matrix. In these systems, in fact, substitutional Mn on the cation sites provides at the same time an efficient hole doping and a localized magnetic moment which couples ferromagnetically with those in the other impurity sites, thanks to a carrier mediated mechanism.¹⁻³ Systems such as GaMnAs, InMnAs, GaMnSb, have in fact received much attention and were thoroughly investigated.⁴⁻⁷

Despite their relevance in present device technology, only very recently the scientific community has been paying attention to transition-metal (TM) doped group IV semiconductors (mainly Si, Ge) and to possible digital alloys based on these compounds. Ferromagnetic (FM) properties up to ≈ 110 K have been reported for MBE-grown MnGe,⁸ along with magnetoresistance phenomena below room temperature, which were partly attributed to Mn_nGe_m ferromagnetic clusters rather than to isolated Mn impurities in the zincblende Ge host.⁹ Recently, a report supported this finding fixing the Curie temperature of the dilute magnetic semiconductor (DMS) at 112 K.¹⁰ Moreover, ferromagnetism at $T_c = 285$ K (Ref. 11) was reported in highly Mn-doped (up to 6%) Ge single crystals obtained by solid solutions, as determined from temperature dependent magnetization and resistance measurements. A later investigation¹² on the same samples showed that the magnetism in Mn_xGe_{1-x} could be, however, due to Mn-rich phase separated regions of the material. Finally, Mn ion-implanted Ge matrix¹³ investigated by means of Kerr effect, showed a magnetic cycle with a coercive field of about 3000 Oe and hysteresis appearing just below room temperature.

From the theoretical point of view, the electronic and magnetic properties of Mn_xGe_{1-x} were investigated by first-principles full-potential linearized augmented plane wave (FLAPW) calculations¹⁴ as a function of the Mn positions in a large supercell. The exchange interaction between Mn ions was found to follow a Ruderman-Kittel-Kasuya-Yoshida (RKKY) behavior as a function of their distance, the estimated Curie temperature¹⁴ ranging from 134 K up to 400 K, in good agreement with experiments.^{8,11}

In previous works^{15,16} some of us investigated Mn impurities in a Ge and Si host matrix at different concentrations and studied the electronic, structural, and magnetic properties of these systems as a function of Mn concentration, with substitutional Mn isotropically diluted in the host compound. Irrespective of the Mn content, we found that the Ge-based systems are very close to half-metallicity and that the effects brought about by Mn impurities have a local character.

Most of the interest on Ge-based possible DMS has been so far limited to doping with Mn or to few other TMs:¹⁷ an extended and systematic study of TM impurities, available for several III-V compounds¹⁸⁻²⁰ but lacking at present for Ge, may help the comprehension of the physical mechanisms determining the magnetic ordering temperature and possibly guide the discovery of even more promising compounds. This paper, therefore, focuses on the extension of first-principles calculations to single impurities of the entire 3d-transition metal series in Ge, and study in detail the energetics of the system, as well as its structural, electronic, and magnetic properties as a function of the different TM atom considered. Due to the delicate balance between structural and magnetic properties, the resulting theoretical description can be affected by the nature of the electron exchange-correlation potential employed within density functional theory. For this reason, we also address the prob-

lem of the exchange-correlation parametrization (LSDA versus GGA) in reproducing and predicting the magnetic properties of these systems, as well as the non-negligible effects of structural relaxation on the final properties of the diluted compounds.

A promising route to enhance the magnetic properties and possibly help solubility has been recently suggested: experimental results demonstrated the possibility of codoping with (Mn, Co) (Ref. 21) and (Mn, Cr) (Ref. 22) impurities in Ge. As the detailed mechanisms governing the codoping of TM's in Ge are still unknown, we also investigate these cases in order to assess whether codoping could make the ferromagnetic coupling stronger or favor incorporation of Mn into the Ge matrix, possibly leading to higher Mn concentrations in the host matrix. To this end, we study the pairing energy for (Mn, Mn), (Co, Co), and (Cr, Cr) on the most favored substitutional sites and compare with those calculated for (Mn, Co) and (Cr, Mn). Our calculations demonstrate that while Mn and Co show strong tendencies towards clustering, Cr does not. Moreover, addition of Co and overall Cr to Mn-doping would oppose to this tendency, thus resulting in a more uniform TM distribution. However, in agreement with experimental findings, both Co and Cr are shown to depress the magnetic properties of substitutional Mn in Ge.

The paper is organized as follows: in Sec. II, we report structural and computational details. In Sec. III, we discuss results regarding the energetics and the structural, electronic, and magnetic properties of a single TM impurity into the Ge matrix, while in Sec. IV we discuss the effect of codoping. Finally, in Sec. V, we draw our conclusions.

II. STRUCTURAL AND COMPUTATIONAL DETAILS

The calculations were performed using the VASP package^{23,24} within local spin-density approximation (LSDA) as well as generalized gradient approximations (GGA)^{25,26} to density functional theory. PAW pseudopotentials²⁷ were used for both Ge and TM atoms, with semicore $3p$ and $3s$ states kept in the core shell. The kinetic energy cutoff used for the wave functions was fixed at 230 eV.

We considered low TM concentrations ($\leq 6.25\%$) corresponding to unit cells containing 32 (64) atoms for the ferromagnetic [antiferromagnetic (AFM) and codoped structures] at the experimental Ge lattice constant ($a=5.636$ Å), well reproduced within LDA (within 0.1%) and less accurately within GGA ($a=5.776$ Å). AFM calculations were performed on the larger cells, with the impurity atoms at the largest distance compatible with the chosen cell (i.e., $a\sqrt{3}$). The irreducible wedge of the Brillouin zone was sampled with several different shells: good convergence was obtained with the (8,8,8) and (4,4,4) shell for the 32 and 64 atom cells, respectively, within the Monkhorst-Pack scheme.²⁸ The TM atom was considered to occupy the substitutional site (i.e., one of the diamond lattice sites) and the interstitial site of the diamond lattice tetrahedrally coordinated. The other possible interstitial site (the one with hexagonal symmetry) was not considered since experimental evidences obtained in similar systems showed that the former site is always favored.^{29,30} Due to the local density underestimate of the Ge band gap,

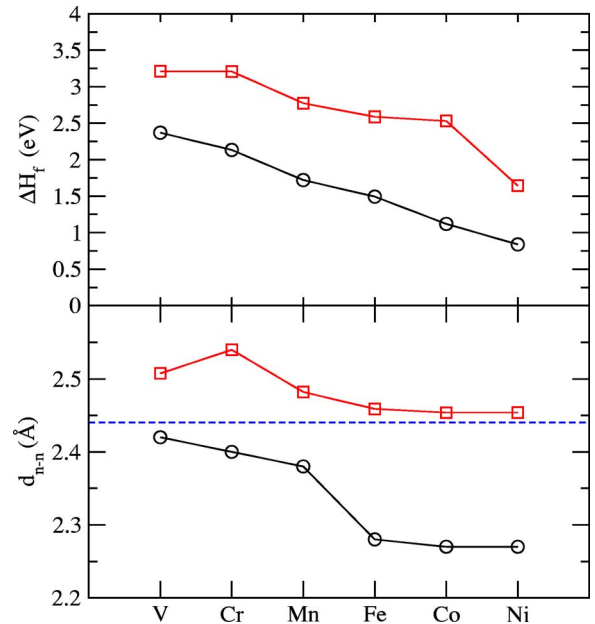


FIG. 1. (Color online) Heat of formation (upper panel) and nearest-neighbor distance (bottom panel) for the substitutional (circles) and interstitial (squares) TM defect in Ge as a function of the TM atomic species. The horizontal dashed line in the bottom panel indicates the ideal Ge-Ge nearest-neighbor distance.

only neutral states were considered in this work for the impurity and this is of course expected to affect the final results, as we will discuss later; however, as shown in other works (see, for example, Refs. 18 and 31) the neutral defect seems to be the lowest possible state for Mn in Ge (Refs. 31 and 32) as well as for several TM impurities in GaAs.¹⁸

III. ISOLATED SINGLE DOPANTS

A. Energetics and structural properties

All the results presented in this work are obtained within GGA and differences and similarities with LSDA, where relevant, are discussed. In Fig. 1 we report the formation energy calculated within GGA for the different TM sites considered within the Ge host matrix. The formation energy is calculated as the energy difference between the total energies of the cell with and without the defect (E_{def} and E_{id} , respectively) considering the chemical potential of the TM atom (μ_{TM}) taken from a metallic reservoir, and the number of substituted Ge atoms, $n^{\text{subst}}=1,0$ for the substitutional and interstitial site, respectively,

$$\Delta H_f = E_{\text{def}} - E_{\text{id}} - \mu_{\text{TM}} + n^{\text{subst}} \mu_{\text{Ge}}. \quad (1)$$

The choice of the reservoir that provides the atomic species needed to form the defect is unfortunately a very delicate issue: the corresponding elemental solids or any compound formed from the considered elements could be a good choice, depending on which one is the most stable at the defined thermodynamical conditions. However, since we are interested in trends and considering the wide variety of TM-Ge compounds that could be stabilized at the thermody-

namical conditions fixed by the growth parameters, we take as chemical potential the value obtained for the corresponding elemental most stable structure of each TM: nonmagnetic bcc V, antiferromagnetic bcc Cr, antiferromagnetic fcc Mn, ferromagnetic bcc Fe, ferromagnetic hcp Co, and, finally, ferromagnetic fcc Ni.

From the results reported in Fig. 1 [panel (a)] we see that the substitutional is favored over the interstitial site for all TM of the $3d$ series. However, the heat of formation keeps being rather large as in other DMS, (of the order of a few eV/atom) for all the species considered, showing that rather low dilution is expected for all the impurities considered. Our results are in fair agreement with previous calculations^{31,32} on Mn in Ge, taking into account the different Ge lattice parameter considered. In addition, the trend of the heats of formation for both substitutional and interstitial sites as a function of the TM atomic species is very similar: it decreases as the $3d$ shell becomes more and more occupied.

In Fig. 1 [panel (b)] we report the TM-Ge distance for both the interstitial and substitutional sites. The substitutional site always results in a bond length contraction with respect to the ideal Ge-Ge distance; at the same time the interstitial site seems to produce larger bond lengths. In this respect, it is useful to mention that LDA calculations find the same trends in bond length as GGA, their values differing of less than 2% for all the TM considered: thus, the TM-Ge bond-length contraction found is not an artifact of GGA which gives a larger Ge lattice parameter than experiment. Similar GGA calculations performed at the Ge GGA-lattice constant still give a TM-Ge bond length reduced by about 2%–3% with respect to the ideal Ge-Ge distance. At variance with experimental results^{11,21,33} claiming that Mn incorporation in Ge results in a dilation of the Ge host lattice, we find a Mn-Ge bond length smaller than the ideal Ge lattice, in good agreement with previous first-principles calculations.¹⁶ It could be argued that local density systematically underestimates bond lengths in magnetic materials³⁴ due to the poor treatment of the correlation in localized d states: if correlations are included within the LDA+ U framework (the standard value $U=3.0$ eV (Ref. 16 was used) we found that the calculated bond length is 2.42 Å, slightly larger than the bare GGA value (2.38 Å) but still not exceeding the Ge-Ge equilibrium distance. This finding establishes that while local density may underestimate by less than 3% the Mn-Ge distances, the calculated bond lengths do not indicate any Ge-lattice expansion. The observed increased $\text{Mn}_x\text{Ge}_{1-x}$ lattice constant reported in the literature agrees with similar findings for other systems [Mn in GaAs and InAs (Ref. 35–37)]: this could possibly suggest that (ii) theory is not well describing the structural properties of the system, or (ii) that Mn occupies interstitial sites or other different positions, or (iii) Mn tends to cluster, thus strongly modifying the host matrix. This issue is still open and requires further theoretical and experimental investigations.

Our results indicate that the heat of formation of a substitutional Mn impurity in the Ge host matrix is higher (by about 1 eV) than the corresponding one for Co; moreover, while the heat of formation of Co in the substitutional site is much lower than in the interstitial site (by about 1.4 eV), for

Mn this energy difference is quite smaller (about 1.0 eV). Therefore, while Co is expected to occupy more likely substitutional rather than interstitial sites (the ratio between the substitutional and interstitial population can be taken as exponentially dependent on the formation energy difference), the same tendency would be strongly reduced for Mn. It is then possible to speculate that Mn would be filling interstitial sites more likely than Co: if this is the case, favored substitutional Co might adjust the strain induced by interstitial Mn. This is however a point which will be discussed in more details later in Sec. IV.

The deformation brought about by the impurity presence fastly decreases away the impurity: in fact, it is already quite small at the second-neighbor shell. We find that the substitutional site induces a deformation of the order of 1%–2% on the second-neighbor shell as well, while the disturbances due to the interstitial site presence are less than 0.5% (not shown). The stability of a defect is in part related to the deformation it produces in the host lattice: while the substitutional site always results in a larger deformation, it is, nevertheless, the most stable site. As a matter of fact, if we only consider the deformation contribution, we find that the elastic energy gain is larger for the interstitial than for the substitutional site (about twice as much). Thus, the total energy gain that favors the substitutional site all over the $3d$ TM series considered is related to a large gain in bonding energy that overcomes the loss in strain energy.

It has been argued³¹ that the preference for the substitutional site in Ge is related to the rather low vacancy formation energy in this material with respect to Si, where Mn is preferentially interstitial. Now, the difference between the interstitial and substitutional formation energy is independent on the chemical potential of the bulk TM atom and should be related to the energy required to create a vacancy in Ge: our results show that this quantity is rather constant over the entire TM series considered; however, the deviations for V and Co (as large as 0.5 eV), show that there is a non-negligible contribution coming from the different bonds established by each TM atom in the substitutional and interstitial position.

B. Properties of TM atoms at substitutional sites

1. Electronic properties

In order to better understand the electronic properties of TM impurities in Ge, it is useful to briefly recall an elementary model, based on simple electron-filling criteria. The electrons which come into play are those belonging to the p states of Ge and to the d and s states of the TM atom, that is from 7 up to 12 electrons for V to Ni. Cubic symmetry splits the fivefold degenerate TM d states into a threefold (t_2) and a twofold (e) degenerate states. The bond between TM and Ge in cubic symmetry is determined by linear combinations of t_2 derived states from the TM and the p states of Ge, having t_2 symmetry as well. The d derived e states do not participate to the bonding due to symmetry rules, and therefore form nonbonding states well localized in energy and space. We can represent schematically the levels as shown in Fig. 2 for the first atom of the series, vanadium. Moving

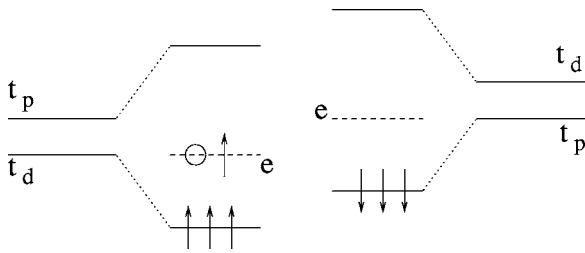


FIG. 2. Simplified schematization of the relative position of the t_2 energy level derived from p , and d states and the e nonbonding states. The filling shown is the one relative to the vanadium case; filling for the other TM considered can be obtained simply adding the correct number of valence electrons.

along the series, the atomic d level becomes more and more deep in energy as it gets more and more occupied; moreover the exchange interaction favors parallel spin alignment up to half-filling. If we now go on and start filling up the levels as sketched in Fig. 2 we would expect magnetic states for V, Cr, and Mn, respectively: in particular we find that the highest occupied states are the e up states for V and Cr while it is a majority t_2 p -derived state for Mn, the minority e state being higher in energy and unoccupied. As we now overcome half-filling of the TM- d shell, we find Fe with its e minority level quite close to the Ge valence band maximum (VBM): the minority e states are now at lower energy than the antibonding t_2 states, so that it becomes more energetically favored to fill in the e down states rather than the antibonding t_2 - p derived states. The filling of the e minority levels results in an equal number of majority and minority occupied states, thus driving the system into a nonmagnetic semiconducting state. Moving to Co and Ni, that is further increasing the d -band filling, the situation is kept almost unchanged from the magnetic point of view. The Fermi level enters the antibonding t_2 states and, since the nonbonding e levels (both majority and minority components) are now completely filled, there is no energy gain in keeping the system spin polarized. Ni impurities are, in fact, nonmagnetic while Co results in a slightly ferromagnetic state due to a Stoner instability linked to a high density of states at the Fermi level (E_F).

This rather simple picture is very well confirmed by the total and the atom-site projected density of states (DOS) for the TM atom, reported in Figs. 3 and 4, respectively. Figure 3 shows how a bare rigid-band approach would not take properly describe the modifications brought about by adding one extra electron to each system to simulate the next TM-atom in the series: the features of the DOS are modified along the series due to the exchange interaction and the hybridization with the Ge- p states. The symmetry-resolved TM $l=2$ contribution to the total density of states plotted in Fig. 4, shows how the energy distance between majority and minority e states, related to exchange interaction, increases from V to Mn and then rapidly decreases as soon as half-filling of the d band is completed (from Fe to Ni), reaching its maximum in Mn, where the e majority states are at energies very close to the bonding combination of t_2 -like states. We find states within the semiconductor band gap (see Fig. 3) in the case of Mn, Co, and Ni, corresponding to the anti-

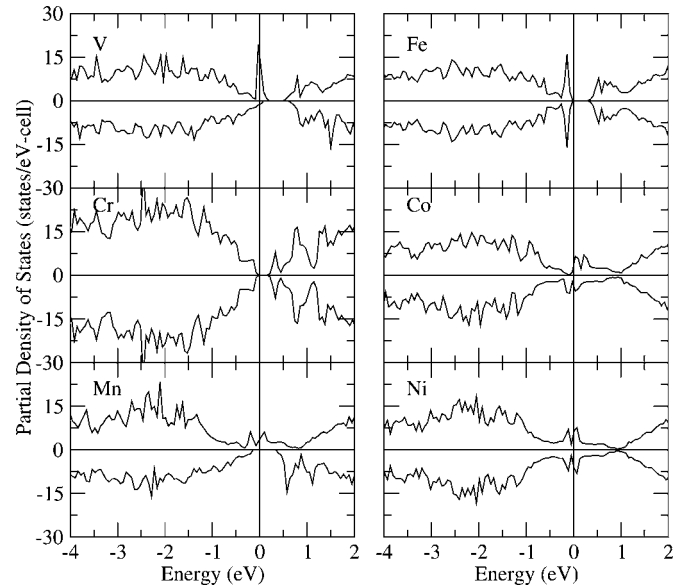


FIG. 3. Total density of states of the $\text{TM}_x\text{Ge}_{1-x}$ system for all the transition metal species considered (TM=V, Cr, Mn, Fe, Co, and Ni). Positive (negative) values refer to up (down) spin component. The zero of the energy scale is set at the Fermi level.

bonding combination of p - d states. p - d hybridization effects are enhanced in the present calculation due to errors of GGA in describing the exchange-correlation interaction for localized states (such as the TM d states); however, we notice that this kind of error has been shown not to dramatically affect the magnetic properties of the materials in GaAs,^{18,38} Si and Ge;^{16,39} we therefore limit our investigation to GGA approximation without introducing empirical U values.

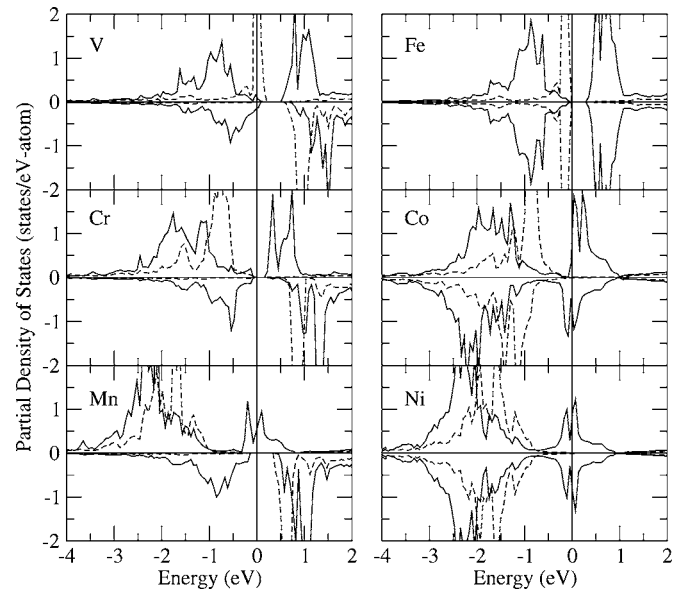


FIG. 4. $l=2$ contribution to the site projected density of states resolved into e - and t_2 -like components (dashed and solid lines, respectively) on the substitutional TM atom for all the transition metal species considered (V, Cr, Mn, Fe, Co, and Ni). Positive (negative) values refer to up (down) spin component. The zero of the energy scale is set at the Fermi level.

TABLE I. Total and TM magnetic moment (in μ_B , within a muffin-tin radius $R=1.27 \text{ \AA}$) calculated within LSDA and GGA as a function of the TM impurity considered.

TM impurity	LSDA		GGA	
	Total	TM	Total	TM
Substitutionals				
V	1.49	1.38	1.36	1.34
Cr	2.00	2.27	2.00	2.28
Mn	3.00	2.78	3.0	2.95
Fe	0.00	0.00	0.00	0.00
Co	0.00	0.00	0.80	0.46
Ni	0.00	0.00	0.00	0.00
Interstitials				
V	1.76	1.18	3.40	2.17
Cr	4.43	3.17	4.35	3.31
Mn	3.22	2.83	3.20	2.95
Fe	2.11	1.93	2.05	1.98
Co	1.03	0.89	0.02	0.05
Ni	0.00	0.00	0.00	0.00

The contribution to the density of states related to p states (not shown) of Ge nearest neighbors of the TM impurity is very similar to that found for Mn in Ge:^{15,16} the larger hybridization between TM- d and Ge- p derived states occurs at lower binding energies (from -1 to -3 eV) and generally shifts towards lower energies as we move from V to Mn along the series, thus following the energy position of the TM t_2 states.

2. Magnetic properties

The magnetic properties of substitutional TM impurities in Ge can be easily inferred from their electronic properties as far as the main trends are concerned. In fact, as we already discussed, we expect stable magnetic states with magnetic moments equals to 1, 2, and $3 \mu_B$ for V, Cr, and Mn, respectively. This is, indeed, what we find as shown in Table I and in Fig. 5, where the calculated magnetic moments (total and on the TM atom) within GGA calculations are reported. First of all, we notice that there is not a large difference between LSDA and spin-polarized GGA results as far as the magnitude of the magnetic moments are concerned; the most striking difference occurs for Co impurity which is found to be nonmagnetic within LDA, while it is FM with about $0.5 \mu_B$ within GGA. This is essentially due to a slightly larger localization of the antibonding t_2 states, which brings the majority component partially below the Fermi level.

However, in order to deeper understand the magnetic properties of these compounds, a more detailed study is needed. This concerns, in particular, the stabilization of antiferromagnetic versus ferromagnetic alignment in V and Cr impurities, both exhibiting e states as the highest occupied states (see Fig. 2). For these two TMs, in fact, we find, that the AFM state is energetically favored over the FM one by ≈ 30 and only 3 meV/TM atom for V and Cr, respectively.

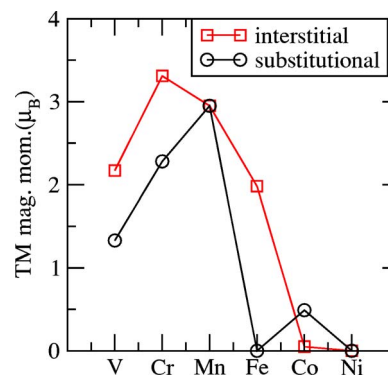


FIG. 5. (Color online) Magnetic moment on the TM impurity, calculated within the muffin-tin radius $R=1.27 \text{ \AA}$, for all the TMs atoms.

This can be understood if we observe (cf. Fig. 2 and Fig. 4) that these are the only two cases in which the e states are those closest to the Fermi level. These states are rather narrow in energy and quite spatially localized since symmetry forbids any hybridization with p -derived states. However, e states interact with other e states at different TM sites, resulting in the small broadening observed in their density of states (Fig. 4). Therefore, we can understand what is happening on the basis of a Hubbard-type picture: we have highly localized states with a very narrow band width, leading to a ground state of the system antiferromagnetic and insulating, since this minimizes the exchange interaction. In the case of vanadium we cannot have an insulator since the states we are considering are the double degenerate e , only partially filled; therefore, we will still have an antiferromagnet but with a metallic behavior. Possible Jahn-Teller distortion might be considered, however, it is reasonable to assume that this effect is rather small. Similar results were found for TM impurities in GaAs (Ref. 18) by means of analogous calculations: in GaAs we have one more electron (three valence electrons from As) to accommodate. Therefore a stable AFM ground state would be expected for V (analogous to Cr in Ge, with the e states as highest fully occupied states), not for Cr (which would correspond to Mn in Ge with magnetic moment close to $3 \mu_B$), and for Fe which is beyond half-filling of the d shell and whose e minority levels are below the hybrid t_2 down states.

The magnetic moment induced on the Ge site which is closest to the TM impurity is always very small (not larger than $-0.02 \mu_B$) and negative: this is already well known in Ge as well as in GaAs and other DMS systems and is related to the p - d hybridization and the antiferromagnetic coupling between localized magnetic moment and semiconducting holes.⁴⁰

An interesting speculation can be done on the basis of our results to infer the behavior of the magnetic properties as a function of TM concentration: as observed in Ref. 41, a more careful investigation requires considering the d - d interaction among TM states, especially when the impurities are close to each other. If the d - d interaction is taken into account, the d -derived t_2 and e states are further split into bonding-antibonding levels. While this interaction is not changing dramatically the state filling of V, Cr, and Mn—since the t_2

bonding states are filled anyway and the antibonding ones for the minority component are empty at quite higher energy—this mechanism may change the filling of the e derived states when they are close to E_F . In fact, when these states are the highest occupied ones, as in the case of Fe, the splitting of the minority e states, could make the system FM with a net magnetic moment, bringing the bonding mixture at lower energy. In fact, Fe in Ge is shown¹⁷ to be FM with $\approx 2\mu_B$ when, at $x=3.125\%$, the Fe atoms occupy nearest neighbor sites of the Ge lattice, and nonmagnetic otherwise. On the other hand, Fe in Ge always shows a FM ground state at $x=6.25\%$.¹⁷

A last interesting comment concerns the properties of the carriers eventually introduced upon TM doping in Ge. The density of states in Fig. 3 shows that the lowest unoccupied states are of the kind e for V, and t_2 for Mn, Co and Ni, while we will not expect, within GGA, any carrier doping effect related to substitutions with Cr, and Fe, both showing a semi-conducting behavior. From this picture, it is clear that the most promising magnetic dopant in Ge is Mn with its high magnetic moment and nominally 2 spin-polarized holes in the delocalized t_2 majority states.

C. Properties of TM atoms at interstitial sites

1. Electronic properties

As we discussed above, the interstitial sites are always less favored than substitutional sites; however, incorporation of TM impurities in interstitial sites has been experimentally demonstrated in GaAs and in several other semiconductor compounds, thanks to kinetic processes and to the formation energy which is not so different between substitutional and interstitial sites for several TM elements. Therefore, it is important to ascertain what is the role played by these defects on the electronic and magnetic properties of the system.

To this end, we report in Fig. 6 the total density of states as well as those projected on the representative l components of the TM impurities. The situation for TM impurities at interstitial sites is rather different from the substitutionals just discussed: still keeping a T_d symmetry, this site is empty in the perfect Ge matrix and has no p states from the nearby Ge pointing towards it. As a result, the TM d states do not mix, or at least interact very weakly, with the t_2 states of Ge: the density of states projected on the $l=1$ component of the nearest neighbor Ge site (not shown) shows that the p states are filled and at lower energy than those induced by the TM impurity, essentially localized close to the Fermi level. Therefore, in order to construct a simplified atomiclike picture in analogy with what done for the substitutional site, we must consider only the TM d electrons (the Ge states are essentially filled and at lower energies) and the crystal-field split t_2 and e states.

The reduced hybridization between TM d and Ge p states stems from the lower density of states at binding energies less than 3 eV. Close to E_F , we can distinguish a small density of states which mimics the shape of the dominant $3d$ states. As we move along the TM series from V to Mn, we find the t_2 and e features moving towards higher binding energies for the majority states; the minority states follow the

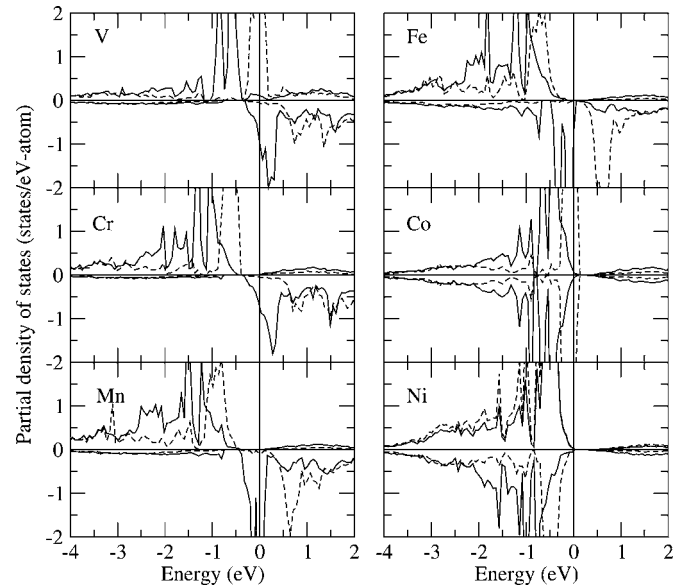


FIG. 6. $l=2$ contribution to the site projected density of states resolved into e - and t_2 -like components (dashed and solid lines, respectively) on the interstitial TM atom for all the transition metal species considered (V, Cr, Mn, Fe, Co, and Ni). Positive (negative) values refer to up (down) spin component. The zero of the energy scale is set at the Fermi level.

same trend separated by the exchange splitting which is approximately the same for e and t_2 states. The Fermi level cuts the e states in vanadium resulting in a possibly unstable state: the ground state for this system could be the +1 charged state, while Cr is rather stable due to the complete filling of the majority e states leading to a rather large magnetic moment. In Mn the atomiclike minority t_2 states keep filling up, and the Fermi level is at the edge of a narrow and high peak: for this TM as well, the neutral state may not be the ground state. In fact, previous calculations performed⁴² on a similar group IV material, i.e., Si, showed that the charged $Q=+2$ state is lower in energy. Moreover, the same considerations done for Mn in GaAs (Ref. 18) would hold in this case, since the electrons from the host are not playing any role in this context. The case of Fe, Co, and Ni follows as a trivial consequence of mere band filling: a rigid band picture would describe the main features except for the exchange interaction which vanishes as we approach complete filling of the atomic d shell in Ni.

2. Magnetic properties

On the basis of the electronic properties just discussed it is immediate to infer the magnetic properties of each TM impurity: we therefore go back to the atomiclike crystal-field split t_2 and e levels, further split by the exchange interaction. Recalling that the number of valence electrons increases from 5 up to 10 going from V to Ni, we have that simple electron counting would predict a magnetic moment of 5, 4, and 3 μ_B for V, Cr, and Mn, respectively; while, for the more than half-filled cases, we should get 2, 1, and 0 μ_B for Fe, Co, and Ni, respectively. We note that these predictions compare quite well with the GGA calculated results reported in

TABLE II. Energetic, structural, and magnetic properties of two TM impurities in substitutional sites in Ge.

	ΔH_f (eV/cell)	Δ_{struct} (eV/cell)	Δ_{pair} (eV/cell)	$d_{\text{Mn-Ge}}$ (Å)	$d_{\text{TM-Ge}}$ (Å)	μ_{Mn} (μ_B)	μ_{TM} (μ_B)	μ_{Tot} (μ_B)
Cr-Cr AFM	4.30	+0.04	+0.06		2.40	2.44	-2.44	0.00
Mn-Mn FM	3.20	0.20	-0.13	2.36		2.98	2.98	6.02
Co-Co FM	1.84	0.35	-0.13		2.25	0.00	0.00	0.00
Mn-Cr AFM	3.72	-0.11	-0.06	2.35	2.43	2.64	-2.76	-0.48
Mn-Co FM	2.55	-0.16	-0.10	2.40	2.23	3.08	0.20	3.47

Fig. 5 (squares), except for V and Cr where hybridization of the t_2 -like states causes a partial filling of the t -minority component. The comparison between LDA and GGA calculated values (cf. Table I) is particularly interesting for V and Cr, where the more effective localization of the d states within GGA brings the e states just at the Fermi level, thus strongly enhancing the density of states at the Fermi level and hindering its possible stability. This mechanism gives rise to a rather high magnetic moment which is of the order of the one estimated from the simple atomic considerations given above. To the high total magnetic moment partially contribute the Ge states and the charge in the interstitial regions. As we observed in discussing the electronic properties, the extremely high density of states at the Fermi level could lead to a charged ground state for V (V^+) with a magnetic moment of $2\mu_B$.

As in GaAs, interstitial Mn in Ge provides high local magnetic moment, but acts as a double donor, with carriers belonging to the t_2 states. Therefore, the presence of Mn in interstitial sites could be detrimental for carrier mediated ferromagnetism, since it would compensate the hole-doping effect of substitutional Mn. However, other configurations should be considered, such as the presence of interacting defects, in order to establish if other mechanisms might occur that would favor ferromagnetism, as recently shown in GaAs.⁴³ The spin polarization of the Ge neighboring sites is parallel to the one on the TM site. While neutral V impurities might be unstable and V^+ doping would result in a very low doping, Cr in interstitial sites is seen to provide rather high local moment (larger than Mn) and t_2 holes: however, its tendency towards AFM alignment would result in a material having a vanishing total magnetization and thus not suitable for spintronic applications.

IV. CODOPING IN GE

A. Energetics and structural properties

One of the major problems that is presently hindering the exploitation of DMS in technological devices is the low temperature at which ferromagnetic order persists in these materials: controlled epitaxial growth techniques have been able to raise the Curie temperature of (Ga,Mn)As up to 170 K, which, however, is still too low to be appealing for technological applications. To this end, several different routes have been investigated in order to (i) maximize Mn dilution into the semiconductor host and (ii) to further increase the effec-

tive carrier number which appears to be very effective in mediating the magnetic interaction. In this context, there have been a few reports^{22,33} of simultaneous growth of Mn with another TM in Ge, namely, Cr (Ref. 22) or Co.³³ While in the former case an enhanced hole concentration was measured that could lead to a more efficient carrier mediated ferromagnetism among Mn impurities,²² in the latter case, Co was added to help solubility of Mn in the Ge matrix thanks to a strain-relieving effect.³³ In both cases, the comprehension of the physical mechanisms driving the impurities localization as well as their energetic and magnetic mutual interactions, is a necessary condition to achieve full control of material design.

As a first step to investigate these mechanisms, we considered the low concentration limit—where only two TM atoms are likely to be close to each other—and performed calculations for two different TM impurities in a 64 atoms Ge cell, both of them on substitutional sites, which we showed to be those energetically favored for all the TM considered. The first TM atom was set at the cell origin, while the other TM atom was considered on a second nearest neighbor site of the Ge lattice and on the farthest site possible [i.e., the site at the $a(1,1,1)$ position of the 64 atoms cell]. In Table II we report the most significant results; in particular, we indicate with ΔH_f the heat of formation of the two TM impurities in Ge, with Δ_{struct} the energy difference between the structure with the impurities far apart and the one with the two TM substitutional impurities as next neighbors, with Δ_{pair} the pairing energy calculated with respect to the ideal Ge lattice and the sum of the total energies of the two isolated TM impurities in a 64 atoms cell (as defined in Ref. 43), with $d_{\text{Mn-Ge}}$ ($d_{\text{TM-Ge}}$) the Mn (TM)-Ge distance, and, finally, with μ the magnetic moments on the respective atomic sites, and μ_{Tot} the total magnetic moment per cell. First of all, we note that the heat of formation for two TM impurities in Ge is larger than twice the single impurity values for Cr, while it is lower for Mn and Co (roughly 0.2 and 0.4 eV/cell, for Mn and Co, respectively). In addition, in the case of two different impurities, we find that the heat of formation of (Mn,Cr) impurities is very close to the sum of the corresponding heat of formation for the single impurities, while for (Mn,Co) codoping we find a lower value (0.30 eV/cell). Now we focus on the pairing energy for the same TM impurity as reported on the first rows of Table II: while in the case of chromium we find a tendency towards large separations between the two impurities (Δ_{pair} is small but positive), for Mn and Co we find the opposite trend.

Thus, Cr doping should result in a more uniformly dilute alloy than using Mn or Co doping: in these last two cases, the system would more likely form regions with higher TM concentration. Moreover, Cr would have AFM ordering while Co and Mn would keep FM alignment. Finally, Co doping is energetically favored over Mn and Cr and has the same tendency to cluster as Mn. Cr doping, on the other hand is energetically very expensive and shows the opposite trend: two Cr impurities will not aggregate, due to the symmetry of the e states involved and to their nonbonding character.⁴³

As we can see from Table II, the lattice relaxations are almost identical to those calculated for the single impurities (cf. Table I) even when the two TM atoms are next neighbors showing that, indeed, the structural relaxation induced by the substitution is very little affected by the TM-TM interaction: the Ge-TM nearest neighbors distances are 2.40, 2.36, and 2.25 Å to be compared with the isolated impurity results 2.40, 2.38, 2.27 Å, for Cr, Mn, and Co, respectively.

We now discuss the cases of (Mn,Cr) and (Mn,Co) codoping which has been experimentally realized. Comparing the last two rows of Table II with the previous ones, we find that simultaneous substitution of Ge with Mn and Cr is energetically favored if the two impurities are substituting on neighboring fcc sites: that is, while Cr itself shows no tendency towards clustering, Mn favors clustering with Cr. In all cases considered, we find that the system gains energy if two TM impurities are next neighbors: the Δ_{struct} value, in fact, is always negative. Moreover, while the Mn-Mn and Mn-Co codoped structures are always ferromagnetic, the Mn-Cr system has the AFM ground state separated by about 20 meV/cell from the FM one. It is interesting to observe that the heat of formation for two different TM impurities substituting on Ge sites is always lower than the heat of formation of the two single impurities (cf. Δ_{pair} in Table II). Thus, the tendency towards metal clustering, as observed in GaAs for the same TM (Ref. 43) persists in Ge (and probably in other semiconductor compounds as well) for different TM and is of the same order of magnitude as the one for similar TM atomic species. Even in this case (see Table II) the lattice relaxations are almost identical to those calculated for the single impurities (cf. Table I).

B. Electronic and magnetic properties

The density of states projected on the relevant l channels of the TM impurity sites and on the Ge atom bridging the two impurity atoms are reported in Fig. 7 for (Mn,Cr) and (Mn,Co) codoping. Comparing the l -projected density of states for the codoped cases, Fig. 7, with those for the single substitutional impurities (Fig. 4), we find rather large similarities: essentially the dominant bonding mechanism is still related to hybridization of t_2 -like states derived from the TM- d and Ge- p orbitals. The bonding among d derived states on different sites is hardly distinguishable on the (Mn,Co) codoping case: only very small differences can be observed comparing the l -projected density of states on the different sites of Fig. 7 with the corresponding ones for the isolated substitutional impurities (cf. Fig. 4). The interaction among d -derived t_2 states on different TM sites is mediated

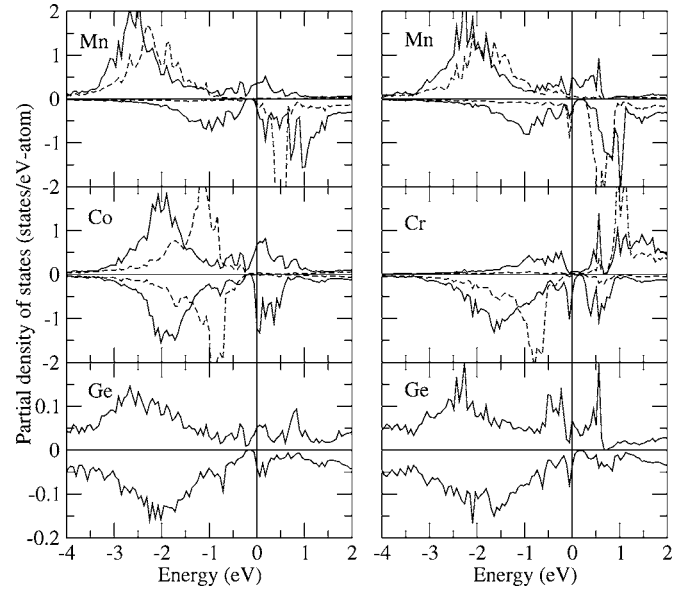


FIG. 7. Site projected density of states on the TM atoms (upper and central panels) and the closest Ge site (lower panel) for the codoped structures considered, (Mn,Co)Ge and (Mn,Cr)Ge on the left-hand and right-hand panel, respectively. Positive (negative) values refer to up (down) spin component. The zero of the energy scale is set at the Fermi level. Symbols as in the preceding figures.

by the Ge p -derived t_2 orbitals which characterizes the bonding as in the single substitution case. On the other hand, more relevant differences can be detected for the (Mn,Cr) codoping case: recalling that the preferred magnetic alignment in this case is antiferromagnetic, we find that the Mn-Cr bond is evidenced by a peak close to the Fermi level on the minority component which has dominant Mn- e and Cr- t_2 character. A corresponding high p density of states is also found on the Ge site bridging the Cr and Mn sites: the Ge p states are in this case mediating a t_2 - e hybridization. Now, Cr would lead to a semiconducting behavior since its localized e majority shell is filled and the antibonding t_2 states are completely empty and pushed at higher energy: this is indeed what happens in the Cr-Cr case where no energy is gained in bringing the two Cr in nearby fcc sites, possibly forming new hybridized states. On the other hand, since Mn has one more electron than Cr, the more delocalized t_2 antibonding states are partially occupied: a new combination of states is formed leading to a lower energy state. Thus, Mn and Cr form new hybridized t_2 - e minority states, thanks to mediation of the bridging Ge p states. This interaction leads to states below the Fermi level in the minority component which lower the occupation of the Mn t_2 up antibonding states and reduce its magnetic moment. The same mechanism would not be energetically convenient for a Mn-Mn interaction or Co-Co as well as Mn-Co, where the system is forced to massively occupy the t_2 antibonding states anyway, due to the larger total number of electrons. In this case, in fact, the higher population of the majority t_2 antibonding states, leads to a slight magnetic moment enhancement: the tendency to cluster is strictly related to stabilization of the magnetic interaction.

This simple picture fully accounts for the magnetic properties observed in the different systems: while the Mn-Mn,

Co-Co, Cr-Cr, and Mn-Co systems show essentially the same magnetic properties of the respective substitutional isolated impurity cases, the Mn-Cr system show AFM alignment with a reduced magnetic moment on Mn ($2.64\mu_B$, to be compared with 2.98 or $3.08\mu_B$ for Mn-Mn and Mn-Co, respectively).

Finally, we can now discuss the comparison, where possible, of our results with experimental findings. The structural results in Table II show that apparently the strain relieving effect invoked in the (Co,Mn) case²¹ should be negligible: the local lattice distortions induced by the presence of two nearby impurities are the same as those due to isolated impurities. However, we find that while two Mn atoms or Co atoms would have the same rather strong tendency towards clustering (their respective pairing energies are very similar, cf. Table II), this tendency is reduced if we mix Co and Mn (the pairing energy in this case is about 30 meV lower). Thus, codoping with Co and Mn would lead to a more even distribution of TM impurities in the Ge host matrix. Moreover, since the heat of formation between substitutional and interstitial sites of Mn isolated impurity is much more similar than in Co, it could be reasonable to expect that Mn would have more chances to occupy interstitial sites than Co: in this last case, there could be an elastic energy contribution since Mn interstitial would locally expand the lattice, while Co substitutional is expected to generate local bond compression. However, (Co, Mn) codoping would end up with a lower total magnetic moment with respect to a full Mn doping: the Co contribution to the total magnetic moment is in fact negligible with respect to the one coming from the Mn atoms.

As far as the (Cr, Mn) codoping is concerned, we find that while Cr shows a tendency towards a more uniform distribution into the Ge lattice, Mn prefers to cluster. In this respect, adding Cr while doping with Mn should favor a more uni-

form TM impurities distribution [the (Cr,Mn) pairing energy is rather low]; however, Cr orders antiferromagnetically and reduces the Mn magnetic moment, thus lowering the total Mn contribution. This is in agreement with the experimental findings²² which found a depression of both magnetization and Curie temperature upon doping with Cr at fixed Mn concentration.

V. CONCLUSIONS

A complete and detailed study of neutral TM impurities in Ge was presented; for all the 3d TM series we studied the structural, electronic, and magnetic properties for substitutional and interstitial sites. A simple analysis in terms of combination of atomic orbitals and electron counting was shown to be very helpful to understand the magnetic properties of the different systems. We showed that Mn in Ge is expected to be the most promising magnetic impurity to obtain spintronic materials, since it is able to ensure the desired ferromagnetic alignment and high magnetic moment. We also studied in detail the tendency towards clustering and the consequent electronic and magnetic properties for two substitutional impurities of the same or different atomic species. We find that while Mn impurities show a tendency to cluster, the presence of Co and overall Cr could favor a more uniform TM impurity distribution. However, both Co and Cr result to be far less efficient than Mn in promoting ferromagnetic alignment and high magnetic moment.

ACKNOWLEDGMENTS

Work supported by INFN through Iniziativa Trasversale Calcolo Parallelo and by Consorzio Gran Sasso through a computing grant at Centro Calcolo dei Laboratori Nazionali del Gran Sasso (INFN).

-
- ¹T. Dietl, H. Ohno, F. Matsukura, J. Cibert, and D. Ferrand, *Science* **287**, 1019 (2000).
²T. Dietl, H. Ohno, and F. Matsukura, *Phys. Rev. B* **63**, 195205 (2001).
³M. Abolfath, T. Jungwirth, J. Brum, and A. H. MacDonald, *Phys. Rev. B* **63**, 054418 (2001).
⁴D. Young, E. Johnston-Halperin, D. D. Awschalom, Y. Ohno, and H. Ohno, *Appl. Phys. Lett.* **80**, 1598 (2002).
⁵H. Ohno, D. Chiba, F. Matsukura, T. Omiya, E. Abe, T. Dietl, Y. Ohno, and K. Ohtani, *Nature (London)* **408**, 944 (2001).
⁶F. Matsukura, H. Ohno, A. Shen, and Y. Sugawara, *Phys. Rev. B* **57**, R2037 (1998).
⁷S. Potashnik, K. C. Ku, S. H. Chun, J. J. Berry, N. Samarth, and P. Schiffer, *Appl. Phys. Lett.* **79**, 1495 (2001).
⁸Y. D. Park, A. Y. Hanbicki, S. Erwin, C. Hellberg, J. Sullivan, J. Mattson, T. F. Ambrose, A. Wilson, G. Spanos, and B. Jonker, *Science* **295**, 651 (2002).
⁹Y. D. Park, A. Wilson, A. T. Hanbicki, J. E. Mattson, T. Ambrose, G. Spanos, and B. T. Jonker, *Appl. Phys. Lett.* **78**, 2739 (2001).
¹⁰A. P. Li, J. Shen, J. Thomsson, and H. Weitering, *Appl. Phys. Lett.* **86**, 152507 (2005).
¹¹S. Cho, S. Choi, S. C. Hong, Y. Kim, J. B. Ketterson, B.-J. Kim, Y. C. Kim, and J.-H. Jung, *Phys. Rev. B* **66**, 033303 (2002).
¹²J. Kang *et al.*, *Phys. Rev. Lett.* **94**, 147202 (2005).
¹³F. D'Orazio, F. Lucari, M. Passacantando, P. Picozzi, S. Santucci, and A. Verna, *IEEE Trans. Magn.* **38**, 2856 (2002).
¹⁴Y. Zhao, T. Shishidou, and A. J. Freeman, *Phys. Rev. Lett.* **90**, 047204 (2003).
¹⁵A. Stroppa, S. Picozzi, A. Continenza, and A. Freeman, *Phys. Rev. B* **68**, 155203 (2003).
¹⁶S. Picozzi, F. Antoniella, A. Continenza, A. MoscaConte, A. Debernardi, and M. Peressi, *Phys. Rev. B* **70**, 165205 (2004).
¹⁷H. Weng and J. Dong, *Phys. Rev. B* **71**, 035201 (2005).
¹⁸P. Mahadevan and A. Zunger, *Phys. Rev. B* **69**, 115211 (2004).
¹⁹K. Sato and H. Katayama-Yoshida, *Semicond. Sci. Technol.* **17**, 367 (2002).
²⁰S. Mirbt, B. Sanyal, and P. Mohn, *J. Phys.: Condens. Matter* **14**, 3295 (2002).
²¹F. Tsui, L. He, A. Tkachuk, S. Vogt, and Y. Chu, *Phys. Rev. B* **69**, 081304 (2004).

- ²²G. Kioseoglou, A. Hanbicki, C. Li, S. Erwin, R. Goswami, and B. Jonker, *Appl. Phys. Lett.* **84**, 4334 (2004).
- ²³G. Kresse and J. Furthmüller, *Comput. Mater. Sci.* **6**, 15 (1996).
- ²⁴G. Kresse and J. Furthmüller, *Phys. Rev. B* **54**, 11169 (1996).
- ²⁵G. Kresse and J. Hafner, *J. Phys.: Condens. Matter* **6**, 8245 (1994).
- ²⁶G. Kresse and D. Joubert, *Phys. Rev. B* **59**, 1758 (1999).
- ²⁷P. E. Blöchl, *Phys. Rev. B* **50**, 17953 (1994).
- ²⁸H. J. Monkhorst and J. D. Pack, *Phys. Rev. B* **13**, 5188 (1976).
- ²⁹K. Yu, W. Walukiewicz, T. Wojtowicz, I. Kuryliszyn, X. Liu, Y. Sasaki, and J. Furdyna, *Phys. Rev. B* **65**, 201303 (2002).
- ³⁰J. Blinowski and P. Kaceman, *Phys. Rev. B* **67**, 121204 (2003).
- ³¹X. Luo, S. Zhang, and S. Wei, *Phys. Rev. B* **70**, 033308 (2004).
- ³²A. da Silva, A. Fazzio, and A. Antonelli, *Phys. Rev. B* **70**, 193205 (2004).
- ³³F. Tsui, L. He, L. Ma, A. Tkachuk, Y. Chu, K. Nakajima, and T. Chikyow, *Phys. Rev. Lett.* **91**, 177203 (2003).
- ³⁴A. Continenza, S. Picozzi, W. Geng, and A. Freeman, *Phys. Rev. B* **64**, 085204 (2001).
- ³⁵Y. L. Soo *et al.*, *Appl. Phys. Lett.* **83**, 2354 (2003).
- ³⁶Y. Soo *et al.*, *Phys. Rev. B* **67**, 214401 (2003).
- ³⁷Y. L. Soo, S. Kim, Y. H. Kao, A. J. Blattner, B. W. Wessels, S. Khalid, C. S. Hanke, and C.-C. Kao, *Appl. Phys. Lett.* **84**, 481 (2004).
- ³⁸J. Park, S. Kwon, and B. Min, *Physica B* **281-282**, 703 (2000).
- ³⁹L. Ottaviano, M. Passacantando, S. Picozzi, R. Gunnella, A. Verna, A. Continenza, G. Bihlmayer, S. Bluegel, G. Impellizzeri, and F. Priolo, *Appl. Phys. Lett.* (to be published).
- ⁴⁰A. Continenza, F. Antoniella, and S. Picozzi, *Phys. Rev. B* **70**, 035310 (2004).
- ⁴¹G. Dalpian, S. Wei, X. Gong, A. da Silva, and A. Fazzio, *cond-mat/0504084* (unpublished).
- ⁴²F. Bernardini, S. Picozzi, and A. Continenza, *Appl. Phys. Lett.* **84**, 2289 (2004).
- ⁴³P. Mahadevan, J. Osorio-Guillen, and A. Zunger, *Appl. Phys. Lett.* **86**, 172504 (2005).